

GSTAR (1,1) Modeling with Time-Correlated Errors for Geoelectric Resistivity Log Data in Pontianak City

Yundari*, Ryan Jonathan and Helmi

Department of Mathematics, Tanjungpura University, Pontianak, Indonesia
Email: yundari@math.untan.ac.id

Abstract

Planting of concrete piles on the soil surface must reach a layer of rock/soil that is hard enough for the building to stand firmly. Rock/soil layers can be studied through geoelectric resistivity log data. We require tools with high prices and need a complicated process to obtain such data. Therefore, a mathematical model is developed to explore geological formations using a space-time model to overcome these problems. The generalized space-time autoregressive (GSTAR) model can be applied to the resistivity data. However, this data correlates with each rock layer. Therefore, we develop a GSTAR model for time-correlated errors. In our study, the parameter index, usually for a concrete time, is applied to the relative time in the form of rock layers. This research uses geoelectric resistivity log data at six locations in Pontianak City, namely Untan 1, Untan 2, Untan 3, Jl. Sawo, Jl KPM Permai, and Gg. Beringin. The GSTAR(1,1) model with time correlation error results in an average RMSE value of 9.51605 Ωm . In addition, we obtain that the most profound peat soil depth is 17.9 m from the surface and is located in the Untan 3.

Keywords: GSTAR (1,1); martingale difference; peat soil; resistivity; time-correlated error.

Abstrak

Penanaman tiang pancang beton pada tanah gambut harus mencapai lapisan batuan/tanah yang cukup keras agar bangunan dapat berdiri kokoh. Lapisan batuan/tanah dapat dipelajari melalui data log resistivitas geolistrik yang memerlukan alat yang mahal dan proses yang rumit untuk mendapatkan datanya. Untuk mengatasi permasalahan tersebut, dibuatlah model matematika untuk mengeksplorasi formasi geologi menggunakan model ruang-waktu. Salah satu model yang dapat diaplikasikan adalah generalized space-time autoregressive (GSTAR). Pada umumnya, data ini memiliki korelasi antarlapisan batuan. Oleh karena itu, pada penelitian ini dikembangkan model GSTAR untuk galat yang berkorelasi waktu. Indeks parameter yang biasanya menggunakan waktu konkret, pada penelitian ini diterapkan pada waktu relatif berupa lapisan batuan. Model ini disebut GSTAR dengan galat berkorelasi waktu. Data yang digunakan adalah data resistivitas geolistrik pada enam lokasi di Kota Pontianak Indonesia yang dinamakan Untan 1, Untan 2, Untan 3, Jl. Sawo, Jl KPM Permai, dan Gg. Beringin. Hasil menunjukkan bahwa model GSTAR(1,1) dengan galat berkorelasi waktu berhasil mengestimasi nilai resistivitas geolistrik di keenam lokasi tersebut dengan nilai rata-rata geometri dari RMSE sebesar 9,51605 Ωm . Selain itu, model ini pun berhasil memperkirakan kedalaman tanah gambut terdalam (dari permukaan tanah) yang terletak di lokasi Untan 3 yaitu 17,9 m.

Kata Kunci: GSTAR(1,1); pembeda martingale; tanah gambut; resistivitas; galat berkorelasi waktu.

2020MSC: 62P30

1. INTRODUCTION

Soil is crucial in construction projects such as roads, buildings, dams, and other structural constructions. The most critical stage in construction activities is to conduct underground observations to estimate building construction design [1]. Various types of soil are used in construction

* Corresponding author

Submitted May 31st, 2022, Revised July 30th, 2022, Accepted for publication July 31st, 2022.

©2022 The Author(s). This is an open-access article under CC-BY-SA license (<https://creativecommons.org/licence/by-sa/4.0/>)

projects, including peat soil. West Kalimantan has 1.8 million hectares of peatland. This soil type can affect building construction due to its extreme softness, unconsolidated, and high water content [2]. In addition, constructing a building on peat soil becomes more difficult because the concrete piles planted must reach a hard layer of rock so that the installation can stand firmly [3].

Layers of soil or rock can be seen from their lithology by analyzing the subsurface conditions in an area. One data that can analyze the subsurface conditions is geoelectric resistivity log data. Geoelectric resistivity log data can be measured using a resistivity meter. However, the tools require high prices and maintenance [4]. Therefore, a mathematical model is needed to predict the value of geoelectric resistivity accurately and efficiently.

One of the models used in forecasting is the space-time model. A frequently used space-time model is called the Space-time Autoregressive (STAR) model. The STAR model can only be used in locations with homogeneous data, assuming the same parameters for each location [5]. This STAR model is further expanded to the Generalized Space-time Autoregressive (GSTAR) model [6, 7, 8]. The GSTAR model has different parameter values at each location. Thus, the parameters of the GSTAR model are more flexible and applicable to heterogeneous locations. The difference between locations is indicated in the form of a weight matrix. This matrix can be determined using uniform, binary, and distance inverses [9] [10] [11].

Several studies applied the GSTAR model. Prameswari et al. [12] [8] analyzed rock resistivity using the concept of anisotropy with the GSTAR model. Yundari et al. [13] performed analysis using a Gamma-Ray log on the GSTAR model with kernel spatial weight, and Jonathan et al. [14] modeled GSTAR(1,1) with independent errors on the geoelectric resistivity data in the Universitas Tanjungpura area. Although the findings of these studies seem promising, they ignored the behavior of the errors in the model. Therefore, this paper intends to fill this gap by performing a GSTAR model that pays attention to the error behavior related to time.

This study uses geoelectric resistivity log data at six different locations in Pontianak City, namely Untan 1, Untan 2, Untan 3, Jl. Sawo, Jl KPM Permai, and Gg. Beringin. We explore geological formations using GSTAR(1,1) model with a weight matrix using the distance inverse method. The time parameter index used in our study is the difference in rock depth. This index follows the superposition principle of stratigraphic analysis, i.e., the bottom rock layer represents the older rock [15]. Forecasting results from the model are then interpreted to see the structure of the soil layer at the observation site.

Estimation errors in the space-time model are generally unaffected by previous estimate errors. There are some cases where the errors do not meet the independence assumption. Therefore, we develop the GSTAR model with the time-correlated errors and the martingale difference process to analyze the geoelectric resistivity log data in Pontianak City.

2. METHODS

GSTAR model with time-correlated errors is performed in this study which consists of nine stages. The first stage calculates the centralized geoelectric resistivity logs data for 6 locations in Pontianak City. The second stage investigates data stationarity in the mean and variance. Differencing and Box-Cox transformation are applied if the data do not appear to be stationarity in mean and variance, respectively. The third stage calculates the GSTAR model's weight matrix using the distance inverse method. The fourth stage estimates the parameters of the GSTAR(1,1) model with

independent errors using the least square method. The fifth stage performs a diagnostic test for the GSTAR(1,1) model with independent errors. The model is good if it satisfies the normality assumption in this test. If the GSTAR(1,1) model with independent errors does not satisfy the normality assumption then re-estimate the parameters of the GSTAR(1,1) model with the time-correlated error using the least square method in the sixth stage. The seventh stage performs diagnostic tests with time-correlated errors. However, if the error model satisfies the normality assumption, we do the next step, i.e., identify the structure of the soil layer. But, if the error model does not meet the normality assumption, it is necessary to analyze further whether the error follows the Martingale difference process. In stage eight, we carry out forecasting using the GSTAR(1,1) model with time-correlated error and evaluate the model based on out-sample data. Finally, in stage nine, the structures of soil/rock layers for 6 locations in Pontianak City are identified based on the forecasting data log resistivity geoelectric model GSTAR(1,1) with time-correlated errors.

2.1 GSTAR(1,1) Model

Let $Z(t)$ be observation data at time t following GSTAR(1,1) process. GSTAR(1,1) model for each location $i = 1,2,3, \dots, N$ and time $t = 1,2,3, \dots, T$ in matrix notation expressed by [9]:

$$\mathbf{Z}(t) = (\Phi_0 + \Phi_1 \mathbf{W})\mathbf{Z}(t - 1) + \mathbf{e}(t) \tag{1}$$

where $\mathbf{Z}(t) = \begin{pmatrix} Z_1(t) \\ Z_2(t) \\ \vdots \\ Z_N(t) \end{pmatrix}$, $\mathbf{e}(t) = \begin{pmatrix} e_1(t) \\ e_2(t) \\ \vdots \\ e_N(t) \end{pmatrix}$, and $\mathbf{W} = \begin{pmatrix} 0 & w_{12} & \dots & w_{1N} \\ w_{21} & 0 & \dots & w_{2N} \\ \vdots & \vdots & \ddots & \vdots \\ w_{N1} & w_{N2} & \dots & 0 \end{pmatrix}$ with $\sum_{j=1}^N w_{ij} = 1$ and $\Phi_k = \text{diag}(\phi_{k1}, \phi_{k2}, \dots, \phi_{kN})$ for spatial order $k = 0,1$ where:

$\mathbf{Z}(t)$: Observation data at time t , where $Z_i(t) = (Z_i(1), Z_i(2), \dots, Z_i(T))$ is a vector $1 \times T$.

$\mathbf{e}(t)$: Observation error at time t , where $e_i(t) = (e_i(1), e_i(2), \dots, e_i(T))$ is a vector $1 \times T$.

i : Observation location, $i = 1,2,3, \dots, N$.

t : Observation time, $t = 1,2,3, \dots, T$.

w_{ij} : Weight of location j to i .

The stationarity of the GSTAR(1,1) model uses the principle of STAR(1,1) stationarity using Theorem 1.

Theorem 1 [16] If all elements Φ_0 and Φ_1 satisfy $|\phi_{0i} + \phi_{1i}| \leq 1$ and $|\phi_{0i} - \phi_{1i}| \leq 1$ for each $i = 1,2, \dots, N$ then GSTAR(1,1), $\mathbf{Z}(t) = (\Phi_0 + \Phi_1 \mathbf{W})\mathbf{Z}(t - 1) + \mathbf{e}(t)$ is stationary.

2.2 Weight Matrix of GSTAR(1,1) Model

The weight matrix used in this study was a weight matrix with the distance inverse method. The distance inverse method is a method that refers to the actual distance between locations. The distance between locations is measured from their latitude and longitude coordinates [17]. In general, the inverse distance weight for each location can be expressed as:

$$w_{ij} = \frac{w_{ij}^*}{\sum_{j=1}^N w_{ij}^*}, i \neq j, \tag{2}$$

where $w_{ij}^* = \frac{1}{d_{ij}}$ and d_{ij} as the distance between location i to location j . Therefore, the distance inverse matrix formed is written as:

$$W = \begin{bmatrix} 0 & w_{12} & \dots & w_{1N} \\ w_{21} & 0 & \dots & w_{2N} \\ \vdots & \vdots & \ddots & \vdots \\ w_{N1} & w_{N2} & \dots & 0 \end{bmatrix}. \tag{3}$$

2.3 Parameter Estimation of GSTAR Model

The GSTAR(1,1) model in Equation (1) can be represented as a linear model as follows:

$$Z = X\Phi + e \tag{4}$$

where, $Z = \begin{pmatrix} Z_1(t)' \\ Z_2(t)' \\ \vdots \\ Z_N(t)' \end{pmatrix}$, $X = \begin{pmatrix} X_1(t) & 0 & \dots & 0 \\ 0 & X_2(t) & \dots & 0 \\ \vdots & \vdots & \ddots & \vdots \\ 0 & 0 & \dots & X_N(t) \end{pmatrix}$, $\Phi = \begin{pmatrix} \phi_{01} \\ \vdots \\ \phi_{0N} \\ \phi_{11} \\ \vdots \\ \phi_{1N} \end{pmatrix}$, $e = \begin{pmatrix} e_1(t)' \\ e_2(t)' \\ \vdots \\ e_N(t)' \end{pmatrix}$, and $X_i(t) =$

$$\begin{pmatrix} Z_i(0) & V_i(0) \\ Z_i(1) & V_i(1) \\ \vdots & \vdots \\ Z_i(T-1) & V_i(T-1) \end{pmatrix} \text{ where } V_i(t) = \sum_{j=1}^N w_{ij}Z_j(t) \text{ for } t = 1, 2, \dots, T; i = 1, 2, \dots, N. \text{ We can}$$

simplify the linear model of Equation (4) into:

$$Z_{(NT \times 1)} = X_{(NT \times 2N)}\Phi_{(2N \times 1)} + e_{(NT \times 1)}. \tag{5}$$

Thus, to estimate the parameters using the least square method of Equation (5) is formulated as follows:

$$\Phi = (X'X)^{-1}X'Z, \tag{6}$$

where $e = Z - X\Phi$ and $X'X$ is a non-singular matrix [18].

2.4 GSTAR(1,1) Model with Time-Correlated Error

For time-correlated errors, the GSTAR(1,1) model is as follows [9]:

$$Z(t) = (\Phi_0 + \Phi_1W)Z(t-1) + \eta(t), \tag{7}$$

where $\eta_i(t) = e_i(t) + e_i(t-1)$ and $\eta_i(t)$ following the martingale difference process. The linear model for estimating the parameters of the GSTAR(1,1) model with the error following the martingale difference process is:

$$Z_{(NT \times 1)} = X_{(NT \times 2N)}\Phi_{(2N \times 1)} + \eta_{(NT \times 1)}. \tag{8}$$

Note that the estimator Φ , is $\widehat{\Phi}_T = (\widehat{\phi}_{01}, \widehat{\phi}_{11}, \widehat{\phi}_{02}, \widehat{\phi}_{12}, \dots, \widehat{\phi}_{0N}, \widehat{\phi}_{1N})'$ satisfy:

$$\mathbf{X}'\mathbf{X}\widehat{\boldsymbol{\Phi}}_T = \mathbf{X}'\mathbf{Z} \tag{9}$$

Then, substitute Equation (8) in Equation (9), that:

$$\mathbf{X}'\mathbf{X}\widehat{\boldsymbol{\Phi}}_T = \mathbf{X}'(\mathbf{X}\boldsymbol{\Phi} + \boldsymbol{\eta}) = \mathbf{X}'\mathbf{X}\boldsymbol{\Phi} + \mathbf{X}'\boldsymbol{\eta} \tag{10}$$

As a result:

$$\mathbf{X}'\mathbf{X}(\widehat{\boldsymbol{\Phi}}_T - \boldsymbol{\Phi}) = \mathbf{X}'\boldsymbol{\eta} \tag{11}$$

which has a solution if the matrix $\mathbf{X}'\mathbf{X}$ is a non-singular matrix.

Vector $\boldsymbol{\eta}$ in Equation (11) is called the time-correlated error vector, and λ is a time-correlated error parameter, defined:

$$\boldsymbol{\eta}_i(t) = \lambda \mathbf{e}_i(t - 1) + \mathbf{v}_i(t). \tag{12}$$

2.5 Rock Resistivity Properties

Rock is a material that has electrical properties. Theoretically, each rock has its electrical conductivity and resistivity value. The same rock does not necessarily have the same resistivity value, and conversely. Different types of rocks can contain the same resistivity value. Factors that affect the resistivity value include mineral composition in rocks, rock conditions, the composition of liquids on rocks, and other external factors [19]. Table 1 shows the range value of rock resistivity [20] [21].

Table 1. Range value of rock resistivity.

Material	Sandstone	Sand	Gravel	Clay	Peat	Groundwater
Resistivity (Ωm)	$1 - 6.4 \times 10^8$	1 – 1000	100 – 600	1 – 100	14.9 – 107	0.5 – 300

3. RESULTS AND DISCUSSION

This study used geoelectric resistivity data in Pontianak City obtained using the OJS Resistivity Meter V-RM 0219. The data was obtained using the electrical resistivity method with Schlumberger configuration. The observation locations and coordinate points are three areas around the Universitas Tanjungpura area (hereinafter called Untan 1 ($0^\circ 03' 09'' S 109^\circ 20' 57'' E$), Untan 2 ($0^\circ 03' 11'' S 109^\circ 20' 54'' E$), and Untan 3 ($0^\circ 03' 06'' S 109^\circ 21' 00'' E$) at Southeast Pontianak District, Gg Beringin ($0^\circ 00' 47'' N 109^\circ 18' 39'' E$) at North Pontianak District, Jl. Sawo ($0^\circ 00' 48'' S 109^\circ 18' 40'' E$) at West Pontianak District, and at East Pontianak District, KPM Permai ($0^\circ 03' 16'' S 109^\circ 22' 37'' E$). The locations of the observation can be seen in Figure 1. Data processing in this study was conducted using Software R. We analyze the geoelectrical resistivity data with 0.1 m different soil depth intervals, i.e., from 0.6 m to 29 m ($T = 285$). A statistic descriptive of the data can be seen in Table 2.

Table 2 shows that the highest mean was located at 11762.52 Ωm in the Untan 3, and the lowest mean was located at 19.89 Ωm in Untan 2 location. Overall, the mean geoelectric resistivity for all locations is greater than the median. It means that the data were clustered around a small resistivity number. Geoelectric resistivity data plots at six locations in Pontianak City can be seen in Figure 2. Figure 2 shows that the data pattern at each location is heterogeneous; therefore, it is appropriate to use the GSTAR model.

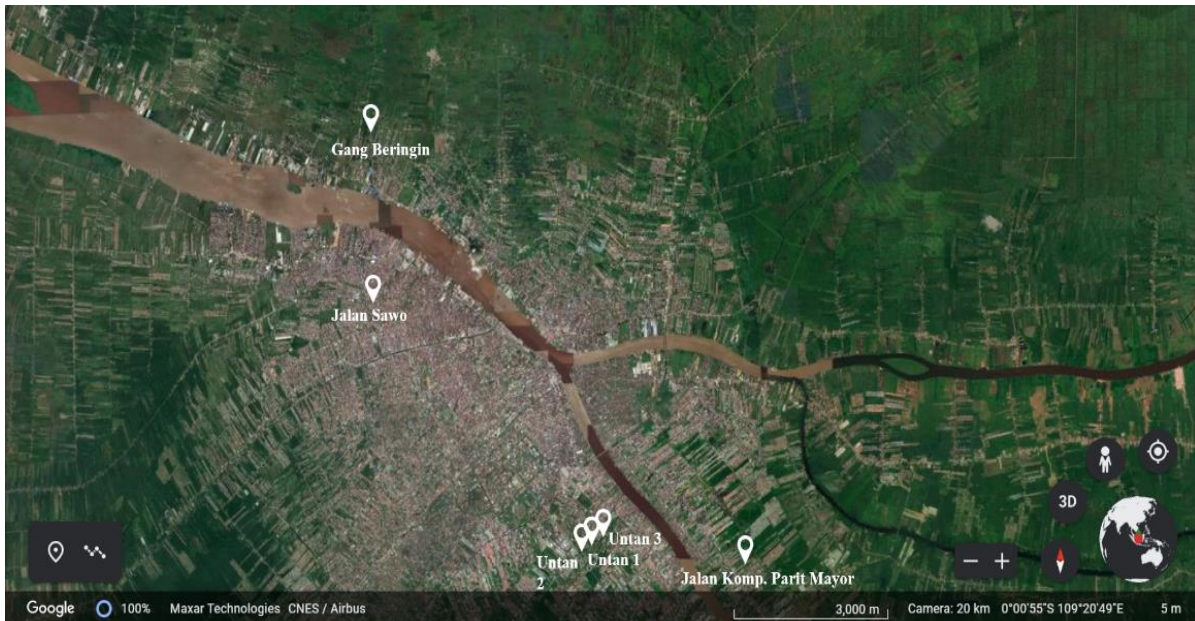


Figure 1. Map of observation locations in Pontianak City.

Table 2. Descriptive statistics of geoelectric resistivity (in Ωm) at six locations in Pontianak City.

Location	Mean	Min	Max	Variance	Standard deviation
Untan 1	29.62	2.85	198.38	2745.63	52.40
Untan 2	19.89	1.73	215.22	913.39	30.22
Untan 3	11762.52	3.00	55038.87	285728295.14	16903.50
Jl Sawo	381.54	1.07	7351.09	1366087.60	1168.80
Jl KPM Permai	203.42	2.46	1020.03	82619.95	287.44
Gg Beringin	67.13	1.93	521.80	16798.34	129.61

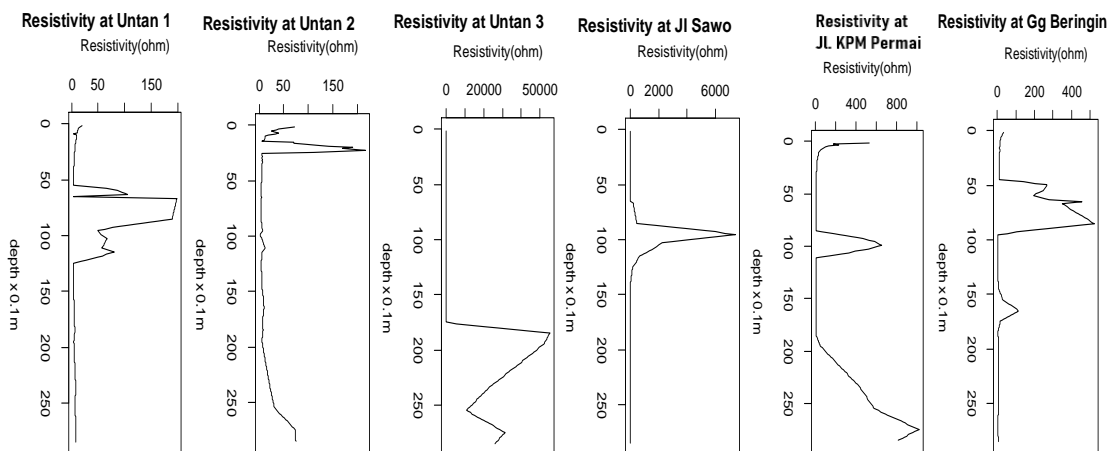


Figure 2. Geoelectrical resistivity plot at six locations in Pontianak City.

3.1 Stationarity Test

Stationarity can be defined as there being no drastic change to the data. The identification of the stationarity of the data can be seen visually through a plot diagram. As shown in Figure 2, the data was not stationary. For that reason, differencing was necessary. The differencing data was then tested using the ADF test. Based on Table 3, the geoelectric resistivity data was stationary and can be modeled.

Table 3. Results of the ADF test for differencing data.

Location	<i>p-value</i>	Explanation	Conclusion
Untan 1	0.01	Reject H_0	Stationary
Untan 2	0.01	Reject H_0	Stationary
Untan 3	0.01	Reject H_0	Stationary
Jl. Sawo	0.01	Reject H_0	Stationary
Jl. KPM Permai	0.01	Reject H_0	Stationary
Gg Beringin	0.01	Reject H_0	Stationary

3.2 Location Weight Determination

The weight matrix with the distance inverse method uses the actual distance value between 6 locations shown in Table 4. The weight matrix is

$$W = \begin{bmatrix} 0 & 0.572137 & 0.396479 & 0.008580 & 0.016695 & 0.006109 \\ 0.683177 & 0 & 0.279730 & 0.010280 & 0.019495 & 0.007318 \\ 0.598344 & 0.353539 & 0 & 0.012916 & 0.025912 & 0.009289 \\ 0.174048 & 0.174638 & 0.173606 & 0 & 0.121443 & 0.356265 \\ 0.273325 & 0.267273 & 0.281096 & 0.098011 & 0 & 0.080295 \\ 0.149500 & 0.149992 & 0.150646 & 0.429827 & 0.120035 & 0 \end{bmatrix}$$

Table 4. The actual distance between locations (in meter).

Location	Untan 1	Untan 2	Untan 3	Jl. Sawo	Jl KPM Permai	Gg Beringin
Untan 1	0	90.42	130.48	6029.37	3098.60	8468.80
Untan 2	90.42	0	220.83	6009.00	3168.80	8441.00
Untan 3	130.48	220.83	0	6044.74	3012.90	8404.40
Jl. Sawo	6029.37	6009.00	6044.70	0	8642.10	2945.60
Jl KPM Permai	3098.60	3168.80	3012.90	8642.07	0	10548.00
Gg Beringin	8468.76	8441	8404.40	2945.56	10548.00	0

3.3 Simulation of Time-Correlation Error Parameter

This simulation was carried out to determine the transformation parameters (λ) in estimating model parameters with time correlation error. This time-correlation error parameter followed the

martingale difference process in Equation (7). The simulation was performed in the range of values of λ between 0.9 and -0.9. Based on the reason for spreading the data, we use starting values of -0.9, -0.5, -0.1, 0.1, 0.5, and 0.9. The simulation results can be seen in Table 5.

From Table 5, the RMSE value gets smaller in parameter estimation if the value of λ is bigger. The greatest RMSE when λ is **-0.9**, and the smallest one when λ is 0.9. Therefore, we used $\lambda=0.9$ to estimate the parameter in the GSTAR model with time-correlation errors.

Table 5. Transformation parameters for estimating model parameters with time-correlation error.

λ	-0.9	-0.5	-0.1	0.1	0.5	0.9
RMSE	77.64641	65.99890	54.35140	48.52770	36.88020	25.23280

3.4 Parameter Estimation of GSTAR(1,1) with Time-Correlated Error

The stationary data was used to calculate the model parameters with the transformation parameter values (λ) of 0.9. The process was calculated using R Software. The parameter estimation results can be seen in Table 6.

Table 6. Parameter estimation of GSTAR(1,1) with time-correlated error.

$\widehat{\phi}_0$	$\widehat{\phi}_1$	$ \widehat{\phi}_0 + \widehat{\phi}_1 $	$ \widehat{\phi}_0 - \widehat{\phi}_1 $
0.70433	0.00001	0.70434	0.70432
0.71805	0.00004	0.71809	0.71801
0.90255	-0.01542	0.88713	0.91797
0.85595	0.00077	0.85672	0.85518
0.73097	0.00055	0.73152	0.73042
0.74502	-0.00240	0.74262	0.74742

Table 6 shows that the GSTAR(1,1) time-correlated error parameter meets the stationary requirements of Theorem 1.

3.5 The result of GSTAR(1,1) Modeling with Time-Correlated Error

The plot of the estimated resistivity values at six locations obtained using the GSTAR(1.1) model can be seen in Figure 3. The red line shows the estimation data, while the black line shows the observation data. The figure shows that the plot of the estimated data has a similar pattern and value that is not much different from the observed data. It indicates that the GSTAR(1,1) model fits well to the data. The RMSE obtained in Table 7 has a relatively small value compared to the range of values in the data. Thus, this model was quite good for estimating the geoelectric resistivity value at each location.

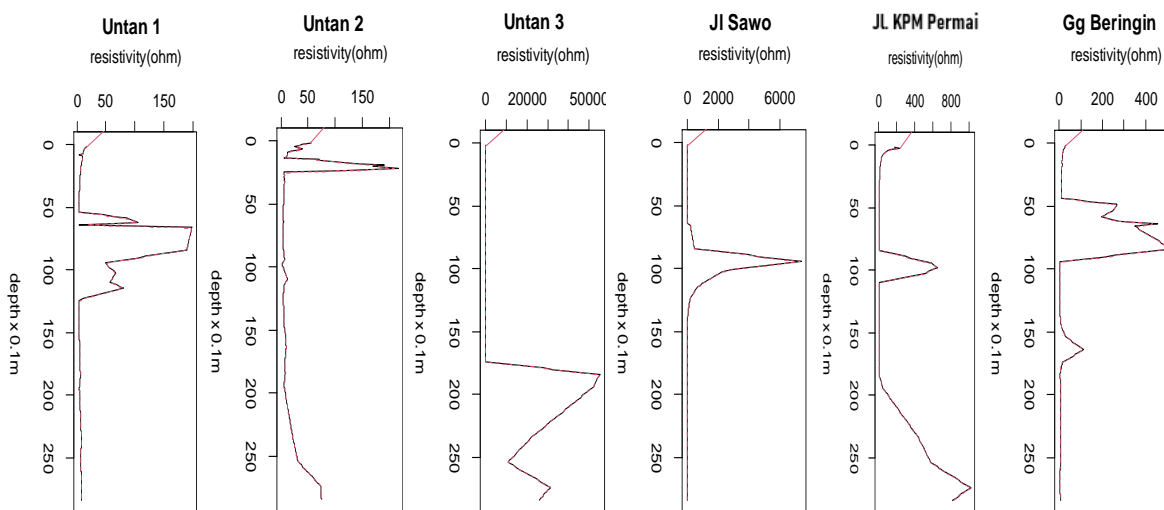


Figure 3. The plot of geoelectrical resistivity estimation vs depth for the GSTAR(1,1) model with time-correlated error.

Table 7. RMSE of the GSTAR(1,1) with time-correlated error at each location.

Location	RMSE
Untan 1	2.99371
Untan 2	3.03070
Untan 3	109.16870
Jl. Sawo	24.53632
Jl KPM Permai	7.69841
Gg Beringin	3.96899
Geometric mean	9.51605

3.6 Diagnostic Test of the Errors of GSTAR(1,1) with Time-Correlated Error

Figure 4 shows the histogram and Q-Q normal plot of the errors. In the above figure, the histogram plot does not have a peak in the middle. The figure below shows that there are still points (data) far from the distribution line. It shows that the errors from the six observed locations are generally not normality distributed. Therefore, the errors in the model do not follow the martingale difference process.

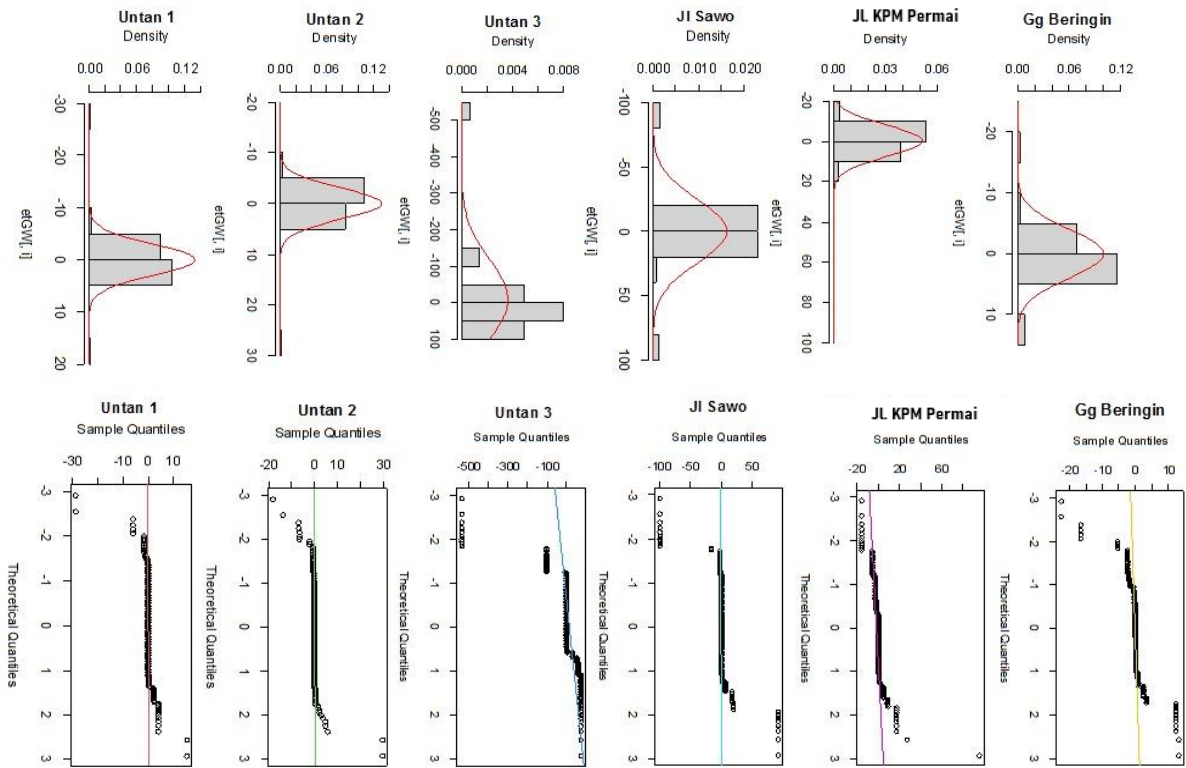


Figure 4. Histogram (above) and Q-Q normal plot (below) of the errors.

Figure 5 shows a correlation value that cannot be ignored in the time lag (more than the significance limit). Thus, it can be concluded that there are other possible processes besides the martingale difference process in this time-correlated error.

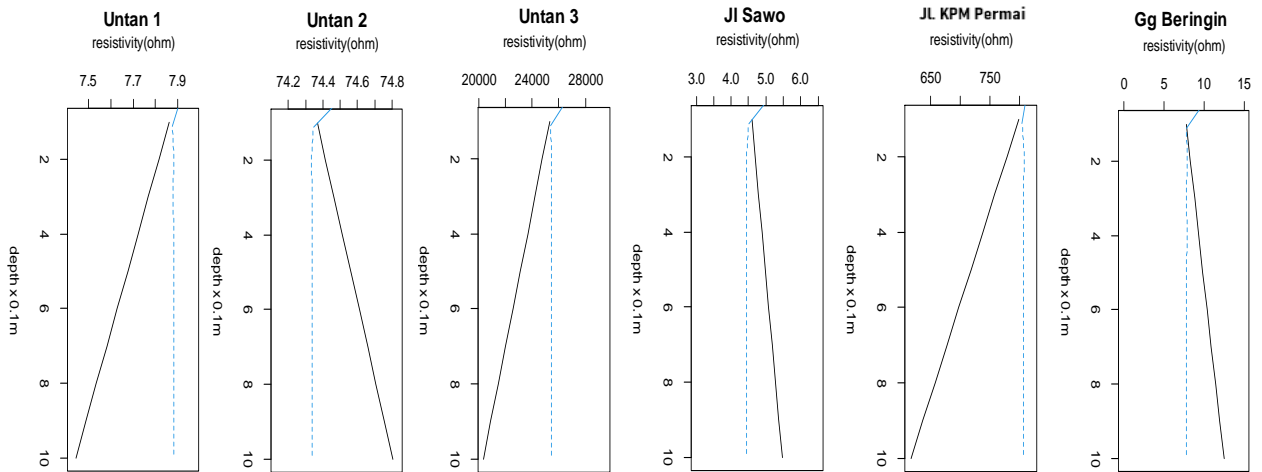


Figure 5. ACF plot for residual model with time-correlation error.

3.7 Forecasting

We used ten samples to forecast the resistivity geoelectric using the GSTAR(1,1) model with the time-correlated error. We compared this forecast with the out-sample data to evaluate the model's

accuracy. Figure 6 illustrates that the GSTAR(1,1) model with time-correlation error can predict the geoelectrical resistivity well at Untan 1, Untan 2, Jl. Sawo, and Gg Beringin. Meanwhile, the model was considered not good in predicting the geoelectrical resistivity at Untan 3 and Jl. KPM Permai. The RMSE of forecasting can be seen in Table 8.

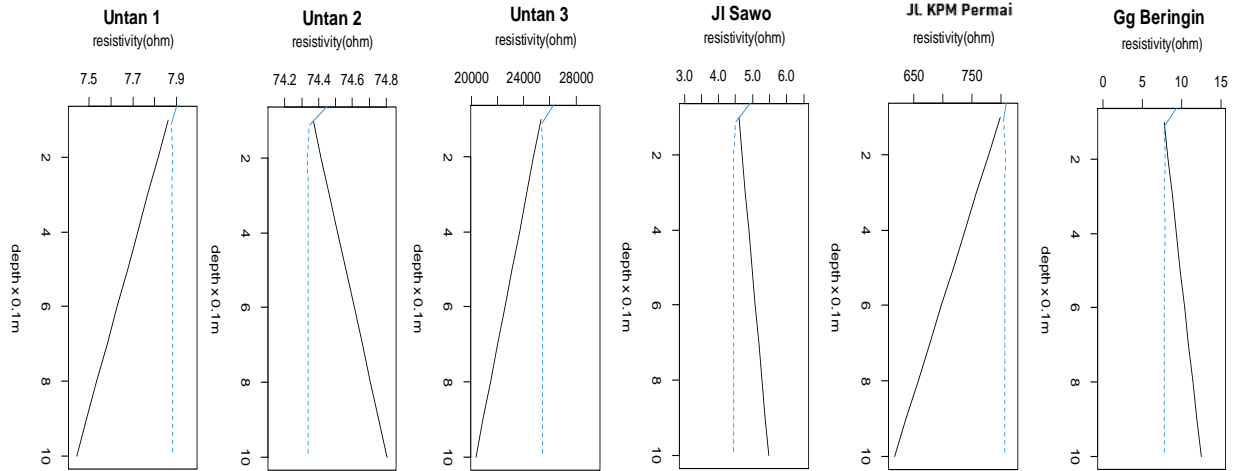


Figure 6. Plot of forecasting value for out-sample geoelectrical resistivity using the GSTAR(1,1) with time-correlation error.

Table 8. RMSE for out-sample geoelectrical resistivity using the GSTAR(1,1) with time-correlated error.

Location	RMSE
Untan 1	0.2638
Untan 2	0.2853
Untan 3	3,036.9600
Jl. Sawo	0.6456
Jl. KPM Permai	114.8272
Gg Beringin	2.7289
Geometric mean	5.99094

3.8 Identification of Rock Layer Structure

The resistivity value obtained from the forecasting results showed that the six observation locations in Pontianak City had a surface layer of peat soil. The depths of the peat soil from the surface for the locations of Untan 1, Untan 2, Untan 3, Jl. Sawo, Jl. KPM Permai, and Gg Beringin were 7.1 m, 2.3 m, 17.9 m, 7.1 m, 9.2 m, and 5.2 m, respectively. The Untan 3 had a reasonably deep peat soil depth of 17.9 m near a swamp area.

Furthermore, this study confirmed that gravel soil could only be found after the peat soil layer. Gravel soil depth for locations of Untan 1, Untan 2, Untan 3, Jl. Sawo, Jl. KPM Permai, and Gg Beringin were found at 7.2 m, 2.4 m, 18 m, 7.2 m, 9.3 m, and 5.3 m. It means that when we construct a building at these six locations, the concrete stakes planted must reach the depth of the gravel soil so that the building can stand firmly.

4. CONCLUSIONS

In this article, we successfully model the geoelectric resistivity log data at six locations in Pontianak City using GSTAR(1,1) with time-correlated errors. This model can be expressed as $\mathbf{Z}_i(t) = (\Phi_0 + \Phi_1 \mathbf{W})\mathbf{Z}_i(t-1)$, where \mathbf{W} is a weight matrix, and Φ_0 and Φ_1 are the time model parameters. The GSTAR(1,1) model with the time-correlated error was satisfactory with a geometric mean of RMSE is 9.51605 Ωm for estimating and a geometric mean of RMSE is 5.99094 Ωm for forecasting the log value of resistivity geoelectric. For further analysis, we found that the error of the GSTAR model was time-correlated but did not follow the martingale difference process. It indicates that there is another type of process for the time-correlated errors in this model. The depths of peat soil from the soil surface for Untan 1, Untan 2, Untan 3, Jl. Sawo, Jl. KPM Permai, and Gg Beringin were 7.1 m, 2.3 m, 17.9 m, 7.1 m, 9.2 m, and 5.2 m, respectively. Meanwhile, gravel soil for the location of Untan 1, Untan 2, Untan 3, Jl. Sawo, Jl. KPM Permai, and Gg Beringin were found at depths of 7.2 m, 2.4 m, 18 m, 7.2 m, 9.3 m, and 5.3 m, respectively.

ACKNOWLEDGEMENTS

We would like to express our gratitude to DIKTI for funding this research project through the PDUPT Scheme for 2019.

REFERENCES

- [1] J. T. D. Goncalves, M. A. B. Botelho, S. L. Machado and L. G. Netto, "Correlation between field electrical resistivity and geotechnical SPT blow counts at tropical soils in Brazil," *Environmental Challenges*, vol. 5, 2021.
- [2] S. Ghareh, S. Kazemian and M. Shahin, "Assessment of compressibility behaviour of organic soil improved by chemical grouting: an experimental and microstructural study," *Geomechanics and engineering: An International Journal*, vol. 21, no. 4, pp. 337-348, 2020.
- [3] Syamsurizal, Cari and Darsono, "Aplikasi Metode Resistivitas untuk Identifikasi Litologi Batuan sebagai Studi Awal Kegiatan Pembangunan Pondasi Gedung," *Indonesian Journal of Applied Physics*, vol. 3, no. 1, pp. 5-10, 2013.
- [4] E. A. Irianto and E. Rahmawati, "Prototipe Alat Ukur Resistivitas Tanah dengan Metode Four-Point Probes," in *Pertemuan Ilmiah XXVIII HFI Jateng dan DIY*, Yogyakarta, 2014.
- [5] P. E. Pfeifer and S. Deutsch, "A Three-Stage Iterative Procedure for Space-Time Modeling," *Technometrics*, vol. 22, no. 1, pp. 35-47, 1980.
- [6] S. A. Borovkova, H. P. Lopuhaa and B. N. Ruchjana, "Generalized STAR Model with Experimental Weights," in *17th International Workshop on Statistical Modelling*, 2022.
- [7] U. Mukhaiyar and U. S. Pasaribu, "A New Procedure of Generalized STAR Modelling using IAcM Approach," *ITB Journal Sciences*, vol. 44A, no. 2, pp. 179 -192, 2012.
- [8] Yundari, U. Mukhaiyar, N. M. Huda, U. S. Pasaribu and K. N. Sari, "Stationary Process in GSTAR(1;1) through Kernel Function Approach," in *IICMA 2019*, Pontianak, Indonesia, 2020.

- [9] Yundari, U. Pasaribu and U. Mukhaiyar, "Error Assumption on Generalized STAR Model," *Journal of Mathematical and Fundamental Sciences*, vol. 49, no. 2, pp. 136-155, 2017.
- [10] N. Nurhayati, U. S. Pasaribu and O. Neswan, "Application of Generalized Space-Time Autoregressive Model on GDP Data in West European Countries," *Journal of Probability and Statistics*, vol. 2012, p. 867056, 2012.
- [11] U. S. Pasaribu, U. Mukhaiyar, N. M. Huda, K. N. Sari and S. W. Indratno, "Modelling COVID-19 growth cases of provinces in java Island by modified spatial weight matrix GSTAR through railroad passenger's mobility," *Helhyon*, vol. 7, no. 2, p. e06025, 2021.
- [12] F. W. Prameswari, A. S. Bahri and W. Parnadi, "Analisa Resistivitas Batuan dengan Parameter Dar Zarrouk dan Konsep Anisotropi," *Jurnal Sains dan Seni ITS*, vol. 1, no. 1, pp. 15-20, 2012.
- [13] Yundari, U. S. Pasaribu, U. Mukhaiyar and M. N. Heriawan, "Spatial Weight Determination of GSTAR(1,1) Model by Using Kernel Function," in *Journal of Physics: Conference Series*, Makasar, 2018.
- [14] R. Jonathan, Yundari, Nurhasanah and O. Y. E. Nada, "Application of GSTAR(1,1) Model for layer peat soil predicted based on resistivity log data," in *Journal of Physics: Conference Series*, BanjarBaru, 2021.
- [15] Britannica, "Law of Superposition," Encyclopedia Britannica, Britannica, 2020.
- [16] S. A. Borovkova, H. P. Lopuhaa and B. N. Ruchjana, "Consistency and asymptotic normality of least squares estimators in generalized STAR models," *Statistica Neerlandica*, vol. 62, no. 4, pp. 482-508, 2008.
- [17] L. A. Faizah and Setiawan, "Pemodelan Inflasi di Kota Semarang, Yogyakarta, dan Surakarta dengan Pendekatan GSTAR," *Jurnal Sains dan Seni Pomits*, vol. 2, no. 2, pp. 317-322, 2013.
- [18] N. F. F. Ilmi, U. Mukhaiyar and F. Fahmi, "The Generalized STAR(1,1) Modeling with time correlated errors to red-chilli Weekly prices of Some Traditional Market in Bandung, West Java," in *AIP Conference Proceedings*, Bandung, 2015.
- [19] M. B. Dobrin and C. H. Savit, *Introduction to Geophysical Prospecting*, McGraw-Hill, 1988.
- [20] J. Milsom, *Field Geophysics*, John Wiley & Sons, 2003.
- [21] L. Ramadhaniningsih and J. Sampurno, "Identifikasi Struktur Lapisan Bawah Permukaan Lahan Gambut di Desa Arang Limbung Kecamatan Sungai Raya Kabupaten Kubu Raya dengan Metode Resistivitas Konfigurasi Dipole-Dipole," *Physics Communication*, vol. 1, no. 2, pp. 29-35, 2017.